Original Research

DIGITAL HEALTH

DIGITAL HEALTH
Volume 9: 1–17

DOI: 10.1177/20552076231203902
journals.sagepub.com/home/dhj

Sage

Significance of platelet adhesion-related genes in colon cancer based on non-negative matrix factorization-based clustering algorithm

Xiao-jv Chi[1,*], Yi-bei Song[1,*], Deng-he Liu[1], Li-qiang Wei[1], Xin An[2], Zi-zhen Feng[3], Xiao-hua Lan[3], Dong Lan[4] and Chao Huang[5]

Abstract

Background: Although surgical methods are the most effective treatments for colon adenocarcinoma (COAD), the cure rates remain low, and recurrence rates remain high. Furthermore, platelet adhesion-related genes are gaining attention as potential regulators of tumorigenesis. Therefore, identifying the mechanisms responsible for the regulation of these genes in patients with COAD has become important. The present study aims to investigate the underlying mechanisms of platelet adhesion-related genes in COAD patients.

Methods: The present study was an experimental study. Initially, the effects of platelet number and related genomic alteration on survival were explored using real-world data and the cBioPortal database, respectively. Then, the differentially expressed platelet adhesion-related genes of COAD were analyzed using the TCGA database, and patients were further classified by employing the non-negative matrix factorization (NMF) analysis method. Afterward, some of the clinical and expression characteristics were analyzed between clusters. Finally, least absolute shrinkage and selection operator regression analysis was used to establish the prognostic nomogram. All data analyses were performed using the R package.

Results: High platelet counts are associated with worse survival in real-world patients, and alternations to platelet adhesion-related genes have resulted in poorer prognoses, based on online data. Based on platelet adhesion-related genes, patients with COAD were classified into two clusters by NMF-based clustering analysis. Cluster2 had a better overall survival, when compared to Cluster1. The gene copy number and enrichment analysis results revealed that two pathways were differentially enriched. In addition, the differentially expressed genes between these two clusters were enriched for POU6F1 in the transcription factor signaling pathway, and for MATN3 in the ceRNA network. Finally, a prognostic nomogram, which included the ALOX12 and ACTG1 genes, was established based on the platelet adhesion-related genes, with a concordance (C) index of 0.879 (0.848–0.910).

Conclusion: The mRNA expression-based NMF was used to reveal the potential role of platelet adhesion-related genes in COAD. The series of experiments revealed the feasibility of targeting platelet adhesion-associated gene therapy.

[1]Department of Clinical Laboratory, The First Affiliated Hospital of Guangxi Medical University, Key Laboratory of Clinical Laboratory Medicine of Guangxi Department of Education, Nanning, China
[2]The First Affiliated Hospital of Guangxi Medical University, Nanning, China
[3]The Second Affiliated Hospital of Guangxi Medical University, Nanning, China
[4]Department of Medical Oncology, The First Affiliated Hospital of Guangxi Medical University, Nanning, China
[5]School of Information and Management, Guangxi Medical University, Nanning, China

[*]These authors contributed equally to this work.

Corresponding authors:
Dong Lan, Department of Medical Oncology, The First Affiliated Hospital of Guangxi Medical University, 6 Shuangyong Road, Nanning, Guangxi Zhuang Autonomous Region, 530021, China.
Email: landong@stu.gxmu.edu.cn

Chao Huang, School of Information and Management, Guangxi Medical University, 22 Shuangyong Road, Nanning, Guangxi Zhuang Autonomous Region, 530021, China.
Email: huangchao@gxmu.edu.cn

Keywords

Platelet adhesiveness, gene, non-negative matrix factorization, transcription factor POU, colon adenocarcinoma

Submission date: 1 March 2023; Acceptance date: 8 September 2023

Background

Platelets are involved in tumor angiogenesis and cancer progression, and high platelet counts in various cancers are associated with shorter disease survival.[1–3] Furthermore, platelets impact the disease burden and treatment outcomes of cancer patients and are involved in cancer progression, including cancer metastasis. Moreover, platelets protect cancer cells from chemotherapy-induced apoptosis and maintain the integrity of the vascular system that supplies the tumor.[4,5] The increase in platelet count has been identified as a predictor of cancer in patients with occult malignancies,[6] and this has consistently been associated with the worsening of progression-free survival and/or overall survival (OS) of patients with ovarian cancer,[7,8] breast cancer,[9] colorectal cancer,[10] lung cancer,[11] and gastric cancer.[12,13]

Neovascularization is essential for tumor growth, in order to ensure a sufficient supply of nutrients and oxygen. Cancer cells usually secrete certain growth factors, such as vascular endothelial growth factor, in order to induce vascularization, and platelets exhibit similar abilities.[14] In addition, platelets release some factors that help maintain the integrity of the microvasculature, which in turn reduces the ability of immune cells to infiltrate tumor tissues, ultimately promoting tumor growth.[15]

The ability to evade attacks by natural killer (NK) cells and fluid shear stress is crucial for cancer cells to successfully metastasize. Cancer cells can accomplish this by adhering to platelets through a process known as platelet cloaking.[16,17] Mice experiments have revealed that reducing the platelet number or function loss of platelets can significantly reduce the ability of cancer cells to metastasize.[18] Meanwhile, the lack of P-selectin (CD62P), which is a cell adhesion molecule in activated platelets, may inhibit intestinal tumor growth by preventing platelet adhesion to tumor cells.[19] These data show that it is possible to develop novel cancer therapeutic strategies by studying platelet adhesion.

The present study aims to identify the molecular clusters of platelet adhesion-associated genes in colon adenocarcinoma (COAD) and investigate the potential mechanisms of action by exploring the association between these identified platelet-associated genes, and tumor growth patterns, clinical efficacies, immune microenvironments, tumor cell stemness, transcription factor regulatory networks, competing endogenous RNA (ceRNA) regulatory networks, and drug sensitivities. The analysis was conducted through multiple dimensions, in order to gain a deeper understanding of the mechanisms of COAD development and identify novel therapeutic targets. Furthermore, a prognostic nomogram was developed to guide future clinical treatments.

Methods

The flowchart for the present study is presented in Figure 1.

Participants

In order to determine the relationship between platelets and OS, the clinical data of COAD patients, who were treated in the First Affiliated Hospital of Guangxi Medical University between January 2017 and December 2022, were collected. In order to detect the mRNA levels, tissue samples were obtained from patients treated in the Department of Medical Oncology of the First Affiliated Hospital of Guangxi Medical University in April 2023. In order to detect the protein levels, tissue samples were obtained from patients, who were treated in the Department of Medical Oncology of the First Affiliated Hospital of Guangxi Medical University between April 2022 and April 2023. The present study was approved by the Ethics Committee of the First Affiliated Hospital of Guangxi Medical University (No. 2023-E186-02), and the privacy of the patients was well-protected. All patients agreed to participate in the study and provided a signed informed consent.

Online data analysis

Online data were used to determine the relationship between the alterations in platelet adhesion-related genes and OS. Initially, platelet adhesion-related genes (Gene Ontology [GO]:0070527, downloaded on 18 July 2022) were obtained from the MsigDB database (http://www.gsea-msigdb.org/gsea/msigdb/index.jsp). Then, the cBioPortal database (http://www.cbioportal.org/) was used to explore the alterations in platelet adhesion-related genes and their effect on survival.

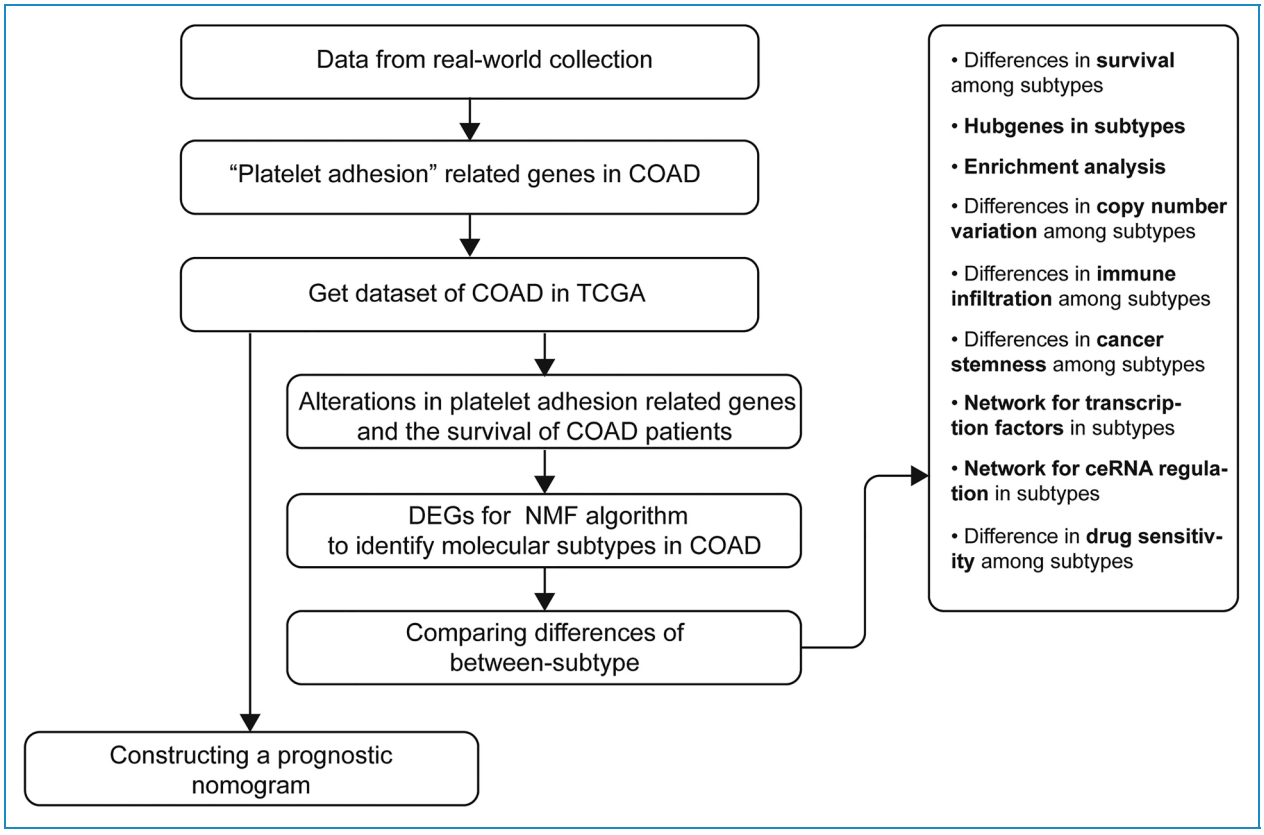

Figure 1. Flowchart for the selection process used in the study.

Downloading of The Cancer Genome Atlas (TCGA) data and bioinformatic analysis

The COAD gene expression matrices for 41 normal and 480 tumor tissues, with the corresponding clinical characteristic data, were downloaded from the TCGA database (https://cancergenome.nih.gov).

In order to determine the role of platelet adhesion-related genes in COAD, a differential analysis was conducted to compare these genes between normal and tumor groups. The differentially expressed genes (DEGs) were defined as false discovery rate (FDR) < 0.05 and $\log_2$ fold change (FC) $> |1|$. Then, the identified genes were subjected to the non-negative matrix factorization (NMF) clustering analysis, in order to determine the corresponding characteristics among the different clusters. Afterward, the OS was compared among clusters using survival curves.

In order to determine the specific differences among clusters, the copy number variants (CNVs) were initially explored, since these have been identified as an important causal factor for various human diseases, and play an increasingly important role in human oncological diseases.[20,21] Then, the patient-related CNV data was downloaded from the TCGA website, and the R software was used to process and visualize the data. Afterward, Kyoto Encyclopedia of Genes and Genomes (KEGG) enrichment analysis was performed for the identified genes using the Database for Annotation, Visualization, and Integrated Discovery (DAVID; https://david.ncifcrf.gov/) tool. Next, a single-sample gene set enrichment analysis was performed to determine the immune infiltration differences among clusters. Then, cancer stemness analysis was conducted to compare the cancer stemness among clusters.

The inter-cluster drug sensitivity analysis was conducted using the R package "oncoPredict," based on the Genomics of Drug Sensitivity in Cancer (GDSC) database (https://www.cancerrxgene.org/).[22]

Hub genes screening and bioinformatic analysis

The hub platelet adhesion-related genes were identified using the gene expression matrix, and these hub genes were defined as FDR < 0.05 and $\log_2$ FC $> |1.0|$.

GO and KEGG functional enrichment analyses were performed for the hub genes using the DAVID tool. Then, the obtained hub genes were subjected to transcription factor enrichment analysis and visualization with R and Cytoscape 3.9.1.

Finally, a predictable ceRNA network was established to identify the ceRNAs involved in the inter-cluster variation. The hub gene targets were initially analyzed using the

ENCORI database, and the remaining genes were filtered according to the survival data ($p < 0.05$). Cytoscape 3.9.1 was used to visualize the data.

Real-time quantitative polymerase chain reaction

Total RNA was extracted from tissues using the VeZol reagent (Vazyme), and the mRNA was reverse transcribed into cDNA using the RevertAid First Strand cDNA Synthesis Kit (Thermo). Next, real-time quantitative polymerase chain reaction (RT-qPCR) was performed using SYBR™ Green PCR reagents (Thermo). The primer sequences used for the present study are presented in Supplemental Table S2. β-actin served as the endogenous reference gene for normalization. The relative expression was calculated using the $2^{-\Delta\Delta Ct}$ method, and each experiment was performed in triplicate.

Immunohistochemistry

The paraffin-embedded fixed tissue was cut into sections. After deparaffinizing the slides for 20 min at 80°C, the slides were immersed in a xylene bath for 5 min, three times. Then, these were rehydrated in 100% ethanol for 30 s, twice, fixed in 95% ethanol for 30 s, and fixed in 75% ethanol for 30 s. Next, antigen retrieval was performed using a repair solution for 3 min in a pressure cooker set at high pressure, and the slides were washed with phosphate-buffered saline (PBS). Then, these slides were immersed in 3% hydrogen peroxide for 10 min, and incubated overnight at 4°C with the appropriate primary antibody (POU6F1, PA5-61403, Invitrogen; MATN3, ab238893, Abcam; ACTG1, ab123034, Abcam; ALOX12, ab211506, Abcam) diluted in PBS. After overnight incubation at 4°C, the slides were rinsed with PBS, and incubated with the appropriate secondary antibody for 30 min at 37°C.

In order to conduct a semi-quantitative analysis of immunohistochemistry, the following criteria were used. Based on staining intensity, the cells were scored as follows: 0 negatively stained, 1 weakly stained (pale yellow), 2 moderately stained (brownish yellow), and 3 strongly stained (sepia). Based on the percentage of positive cells, the positive ratio scores are as follows: 1, 25% or less; 2, 26%–50%; 3, 51%–75%; 4, 76% or more. We calculated the final score by multiplying staining intensity scores and positive ratio scores.

Nomogram construction and verification

Least absolute shrinkage and selection operator (LASSO) Cox regression analysis was initially performed for the platelet adhesion genes, in order to identify the genes related to the prognosis. Then, the screened genes were subjected to univariate analysis, and all significant variables obtained from the univariate analysis were entered into the multivariate analysis (Supplemental Figure S1). All included variables met the proportional risk assumption, based on the log survival plot. The prognostic factors were identified according to the forward stepwise Cox proportional risk regression model, and a nomogram was constructed. Then, the nomogram was validated through discrimination and calibration. The model discriminative power was assessed using Harrell's consistency (C) index, which handles censored data, and estimates the probability of events. A higher C index indicates better discriminative power. The differences between the predicted and actual survival rates were compared using calibration plots.

Statistical methods

For the survival analysis of real-world data, all analyses were conducted using the limma, survival, or survminer packages in R (version 4.2.1). The patients were divided into high and low groups, according to the median platelet count, which was set as the cutoff value in the survival analysis. The statistical analysis was conducted using the R software (version 4.2.1), and data visualization, nomogram construction, and nomogram validation were performed. The p-values were determined using Student's t-test or analysis of variance. A p-value of <0.05 was considered statistically significant.

Results

Platelet count and its correlation with OS in COAD patients

A total of 945 patients from real world met the inclusion criteria, and these were used for the analysis. Among them, 46 were at Stage I, 285 at Stage II, 272 at Stage III, and 342 at Stage IV. There was a significant difference in platelet count across the tumor pathologic stages. The median value was 233.4×10^9/L in Stage I, 269.8×10^9/L in Stage II, 307.8×10^9/L in Stage III, and 374×10^9/L in Stage IV. The results presented in Figure 2 show that the platelet count was proportional to the pathologic stage at presentation (Figure 2(a)). Furthermore, the OS was inversely correlated with the platelet count (Figure 2(b), $p < 0.001$).

Alterations in platelet adhesion-related genes inversely correlate with OS

A total of 70 genes involved in platelet adhesion were identified from the MsigDB database. The expression of these 70 genes was compared between the COAD and control samples using the cBioPortal database. A total of 1471 samples from four studies were included for the analysis: 619 studies from the Dana-Farber Cancer Institute (DFCI; Cell Reports, 2016), 74 studies from Genentech (Nature 2012), 640 studies from The Cancer Genome Atlas (TCGA; Firehose Legacy), and 138 studies from

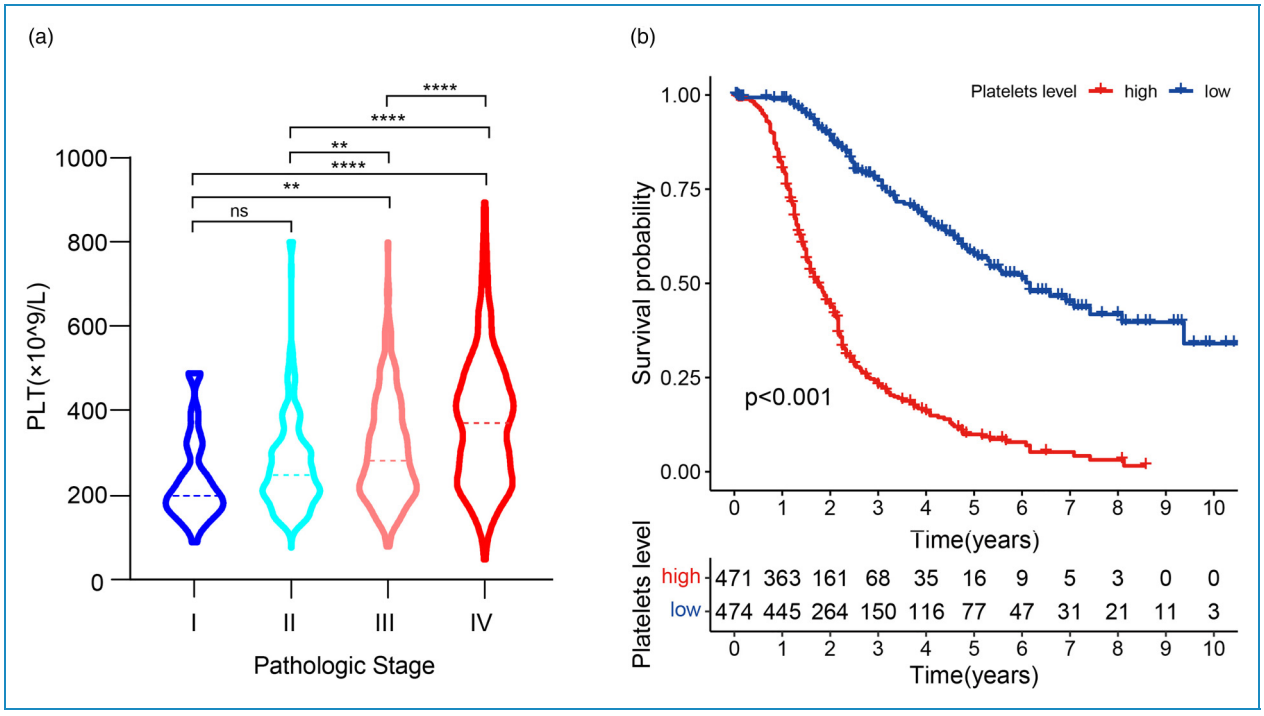

Figure 2. The association between platelet counts and the clinicopathological stage or survival. (a) The distribution of platelet counts in patients in different pathological stages. (b) The Kaplan–Meier survival curves between groups with high and low platelet counts (ns, $p > 0.05$, *$p < 0.05$, **$p < 0.01$, ***$p < 0.001$, ****$p < 0.0001$).

Memorial Sloan Kettering (MSK; Genome Biol 2014). Then, the genetic alterations in platelet adhesion-related genes were explored. Mutations were identified in all four studies, while amplifications, profound deletions, and multiple alterations were only identified in the TCGA data. These mutations were the most prevalent genetic alterations in studies from DFCI, Genentech, and MSK, while amplification was the most prevalent in studies from TCGA (Figure 3(a)). The survival analysis revealed that the alterations in platelet adhesion-related genes inversely correlate with OS (Figure 3(b), $p < 0.001$).

Differentially expressed platelet adhesion-related genes and characteristics of patients with different DEGs

Using the data downloaded from the TCGA database, 23 DEGs were identified: ADAMTS18, BLK, CEACAM1, COMP, CSRP1, CTSG, FGA, FGB, FGG, FLNA, HBB, ILK, ITGB3, MMRN1, MYL9, P2RY12, PDPN, PIK3CG, SERPINE2, SLC7A11, STXBP1, TYRO3, and WNT3A. These DEGs are presented in the heatmap in Figure 4.

The further NMF clustering analysis of these 23 DEGs revealed two unique clusters of 433 COAD patients from TCGA, with 54 patients in Cluster1 and 379 patients in Cluster2 (Figure 5(a)). The survival curves were drawn by matching the survival data for each patient. The results revealed that the OS of patients was better in Cluster2, when compared to Cluster1 (Figure 5(b)).

Difference in CNVs between clusters

The analysis of CNVs in the two clusters revealed that 16 platelet adhesion-related genes had greater copy number gain than loss (GNAS, MYL9, PPIA, IL6, ACTG1, PRKCA, WNT3A, ACTB, C1QTNF1, COMP, EMILIN2, GATA1, ITGB3, SYK, TLN1, and VCL), and 30 genes had greater copy number loss than gain (LYN, PTPN6, CEACAM1, FGA, FGB, FGG, GP6, METAP1, MMRN1, SLC7A11, ACTN1, ALOX12, BLK, BLOC1S4, CELA2A, CSRP1, DMTN, HBB, IL6ST, ILK, MYH9, PDPN, PIK3CB, PRKCD, PRKCQ, PRKG1, SH2B3, STXBP3, TSPAN32, and TYRO3) in Cluster1 (Figure 6(a)). In Cluster2, 29 genes had greater copy number gain than loss (ACTG1, GNAS, MYL9, C1QTNF1, CD9, PRKCA, PTPN6, ACTB, F11R, MPL, VCL, PEAR1, CLIC1, CSRP1, IL6, EMILIN2, PRKCQ, FLNA, MYL12A, PPIA, TSPAN32, MYH9, P2RY12, PIK3CB, RAP2B, PDGFRA, TLN1, ITGB3, and PLEK), and 36 genes had greater copy number loss than gain (LYN, GP6, PRRG1, CELA2A, IL6ST, PDPN, PIK3CG, FN1, SERPINE2, WNT3A, ABAT, BLOC1S4, JAK2, STXBP3, CEACAM1, HBB, STXBP1, ALOX12, BLK, HSPB1, ILK, MMRN1, SH2B3, SLC7A11, TYRO3, UBASH3B, COMP, DMTN, FGA, FGB, FGG, METAP1,

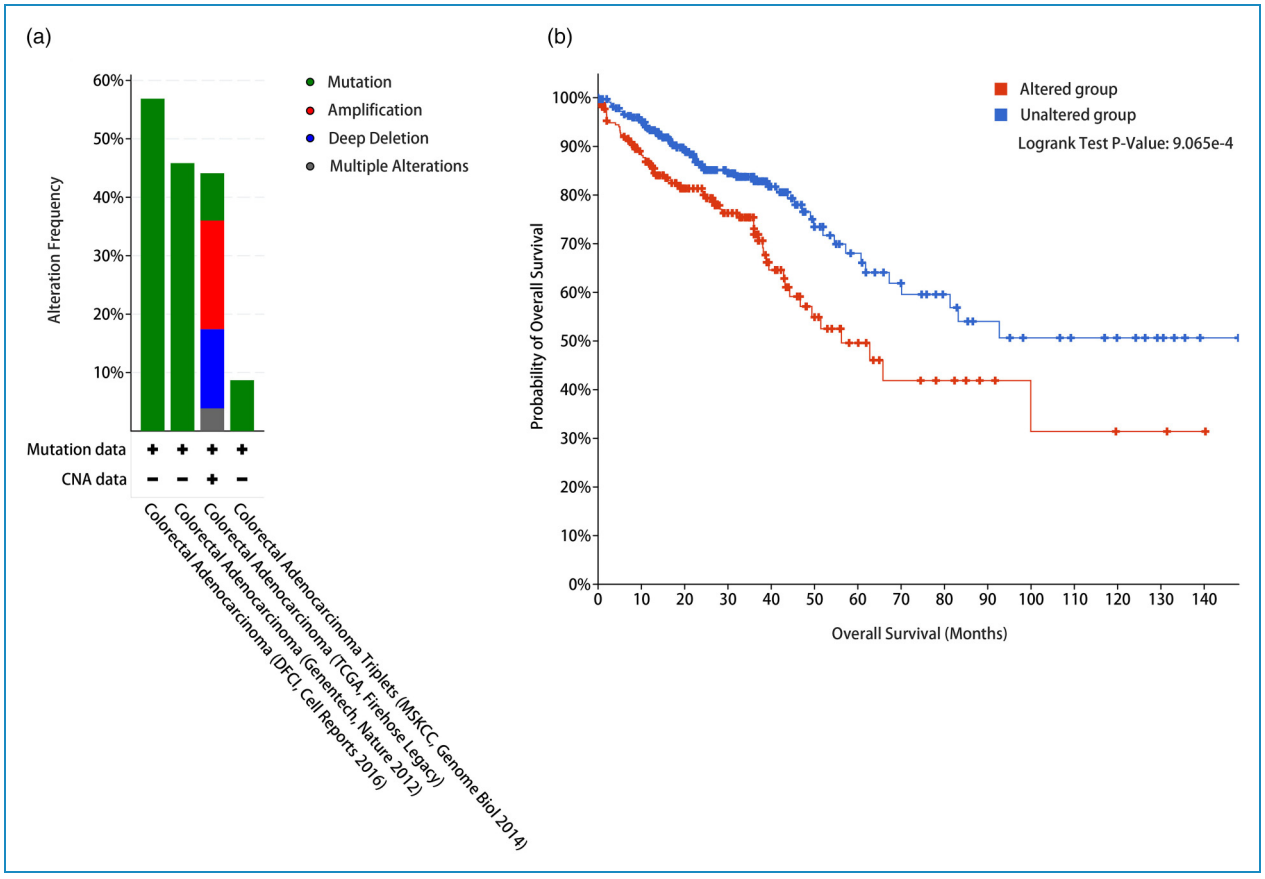

Figure 3. Genetic alteration mining and survival analysis. (a) The alterations of the 70 platelet adhesion-related genes were explored in four different colon adenocarcinoma (COAD) study cohorts. (b) The Kaplan–Meier survival curves between groups, with and without alterations ($p < 0.001$).

PRKCD, ADAMTS18, FERMT3, and FIBP) (Figure 6(b)). Next, a further KEGG enrichment analysis was conducted for these genes with changed copy numbers. The results revealed that genes with increased CNVs in Cluster1 were mainly enriched in the Rap1 signaling pathway, leukocyte transendothelial migration, and the PI3K-Akt signaling pathway (Figure 6(c)). Furthermore, genes with decreased CNVs in Cluster1 were mainly enriched in the B cell receptor signaling pathway, Fc gamma R-mediated phagocytosis, and the T-cell receptor signaling pathway (Figure 6(d)). The increase in CNVs in Cluster2 mainly concentrated in leukocyte transendothelial migration, the Janus kinase-signal transducers and activators of transcription signaling pathway, and the PI3K-Akt signaling pathway (Figure 6(e)). The decrease in CNVs in Cluster2 was primarily concentrated in the chemokine signaling pathway (Figure 6(f)).

Differences in immune infiltration and cancer stemness between clusters

Next, the immune infiltration and activity in tumors were quantified between the two clusters. The results revealed that five immune cells were significantly different between the two groups (Figure 7(a)): incompletely mature NK cells ($CD56^{bright}$), fully mature NK cells ($CD56^{dim}$), gamma delta T cells, T helper (T_h)17 cells, and T_h2 cells. Furthermore, tumor stem cells were the most important cause of treatment failure in malignant tumors.

In order to understand the differences in cancer stemness between the two clusters, the cancer stemness index was explored. This index was used to assess the similarity of tumor cells to stem cells, since having an active biological process similar to stem cells would result in a higher degree of tumor dedifferentiation. The analysis results revealed that cancer stemness was higher in Cluster2, when compared to Cluster1. However, the survival rates were better in Cluster2, when compared to Cluster1 (Figure 7(b)).

Differences in drug sensitivity between clusters

In order to determine the sensitivity of each cluster to various oncology drugs, and provide a reference for clinical treatment, the drug sensitivity difference between the two clusters was further analyzed. A total of 13 drugs with

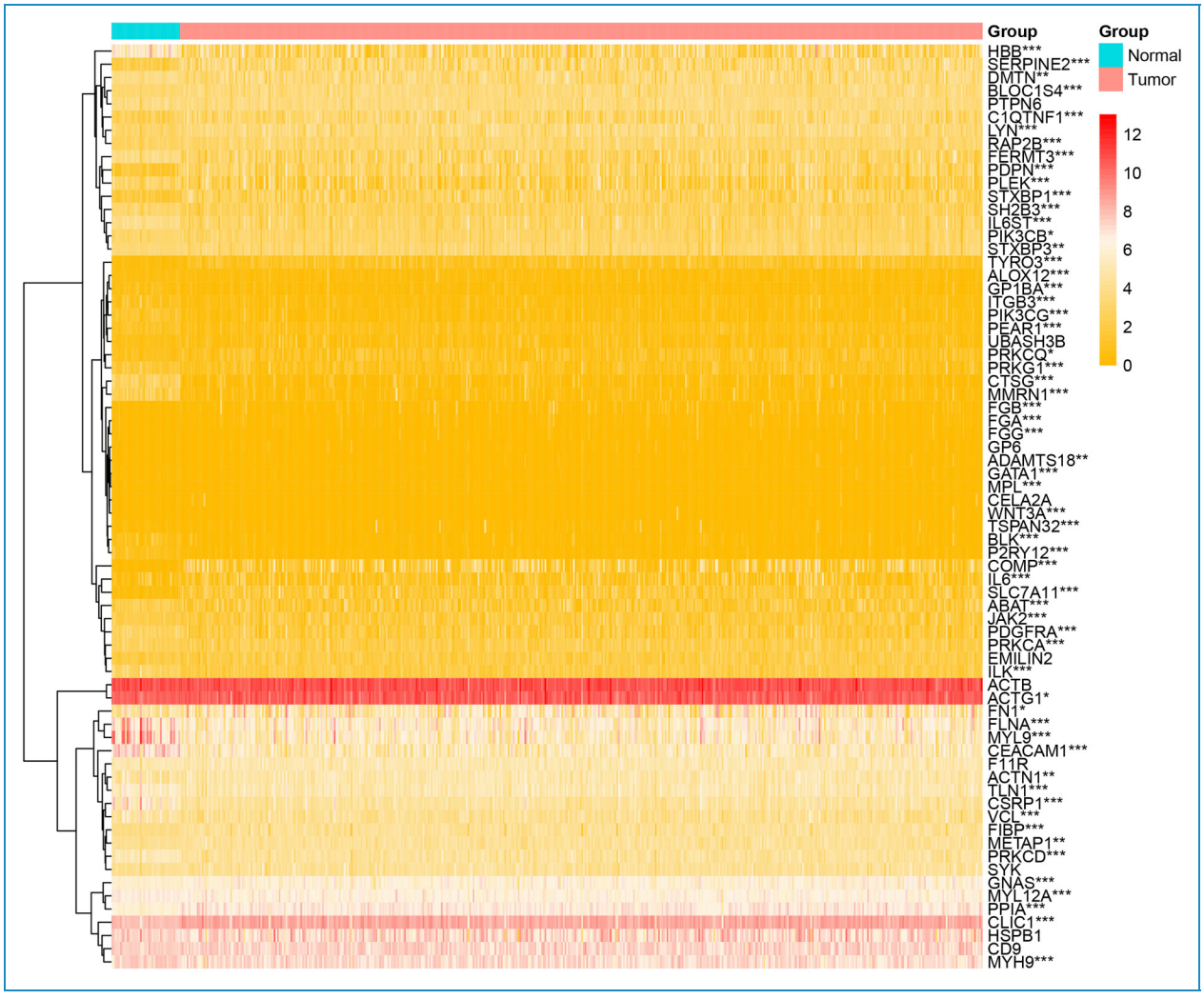

Figure 4. Heatmap for the 70 platelet adhesion-related genes (the DEGs are marked in dark blue color).

significant differences were identified (Figure 8 and Table 1): alisertib, crizotinib, dabrafenib, Eg5_9814, elephantin, epirubicin, ERK_2440, ERK_6604, PAK_5339, PD0325901, SCH772984, trametinib, and ulixertinib. According to the analysis results, Cluster2 responds better to treatment with the above-mentioned drugs, when compared to Cluster1.

Identification of hub genes and enrichment analysis

A total of 16 hub genes were obtained, based the criteria of FDR of <0.05 and $\log_2$ FC >|1.0|: MATN3, SPACA3, MICU3, ZFP37, RIPPLY3, LY6G6F-LY6G6D, COMMD7, CHN2, DCN, BCHE, PRAMEF12, ZNF461, EMCN, CD36, GPRC5D, and CCDC152. As shown in Figure 7(c), 15 of these genes were downregulated, and one gene was upregulated. The GO enrichment analysis of these hub genes revealed that the main molecular function involved the extracellular matrix structural constituent, amyloid-beta binding, Toll-like receptor binding, and low-density lipoprotein particle receptor activity (Figure 7(d)). The KEGG enrichment analysis revealed that these genes are involved in the adipocytokine signaling pathway, cholesterol metabolism, fat digestion, and absorption (Figure 7(d)). The transcription factor analysis (Figure 7(e)) revealed the enrichment of POU6F1 (POU class 6 homeobox 1). The established ceRNA network revealed that one gene (MATN3), three miRNAs (hsa-miR-577, hsa-miR-20a-5p, and hsa-miR-186-5p), and 23 lncRNAs (DUBR, MIR99AHG, AC127070.2, LINC02381, AC015712.2, AC015871.3, AL031123.2, PINK1-AS, LINC02035, AL157392.3, ARRDC1-AS1, THAP7-AS1, SGMS1-AS1, AC008393.1, BOLA3-AS1, NIFK-AS1, OIP5-AS1, ARHGAP5-AS1, LINC01128, SCAMP1-AS1, ARMCX5-GPRASP2, and ERVK13-1) were involved in the inter-cluster variation.

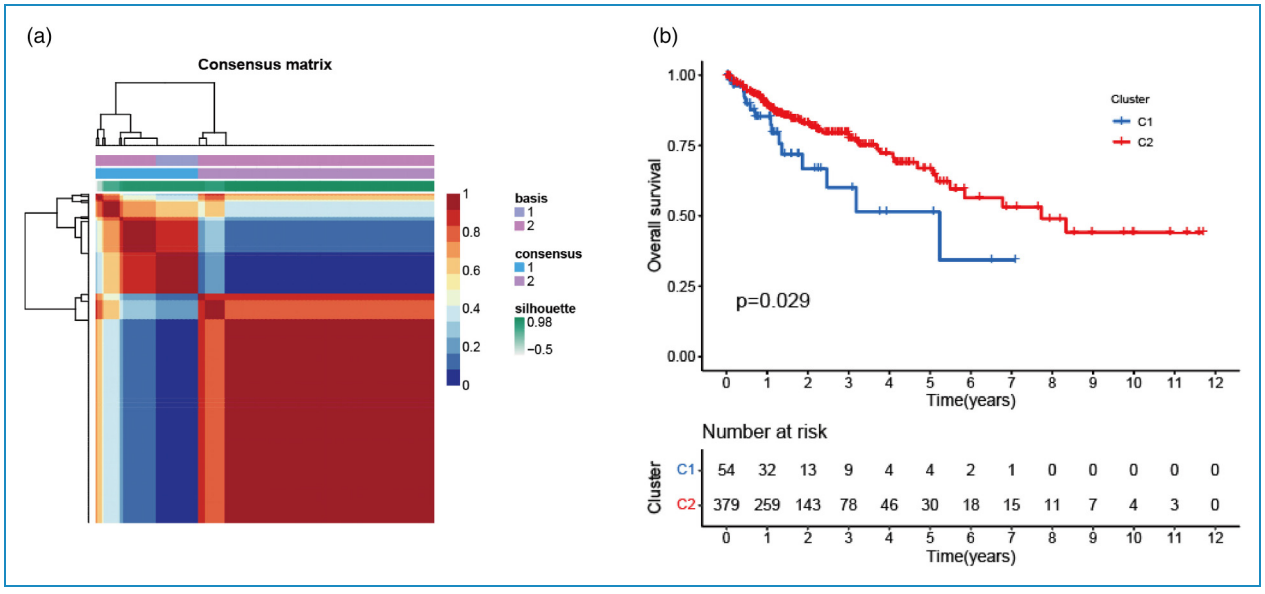

Figure 5. Identification and survival comparison of Cluster1 and Cluster2. (a) Two clusters were identified through non-negative matrix factorization (NMF). (b) The Kaplan–Meier curve for Cluster1 and Cluster2.

Inter-cluster transcription factor regulatory network

Transcription factors control chromatin accessibility and transcription by recognizing specific DNA sequences and forming complexes to direct the gene expression. The results would lead to DNA-binding transcriptional repression activity, RNA polymerase II specificity, and sequence-specific double-stranded DNA-binding activity. In addition, these are involved in the negative regulation of transcription by RNA polymerase II.

Nomogram construction and verification

LASSO logistic regression analysis was performed to select the important predictive features in platelet adhesion-related genes and prevent overfitting (Figure 9(a)). A total of seven genes were selected using the LASSO logistic regression algorithm (the specific LASSO coefficients of genes are presented in Supplemental Table S2). Then, the biomarkers that improved the prognosis of COAD were assessed by univariate and multifactorial analyses, according to $p < 0.05$, and the prediction model was established (Figure 9(b)). Two platelet adhesion-related genes, ALOX12 and ACTG1, were included. The clinical features (primary therapy outcome and pathologic stage) were also included in the prognostic model of Harrell's C index, and these were used to evaluate the discriminatory power of the model (0.879 [0.848–0.910]). The nomogram presented in Figure 9(e) was based on the results of this model and was created to predict the one-year and three-year OS rates. The calibration plots presented in Figure 9(f) reveal the excellent calibration of the nomogram, and the receiver operating characteristic (ROC) curves for the nomogram for OS (area under the curve [AUC] for one-year = 0.749, AUC for three years = 0.712). Furthermore, compared to the other prognostic models in the four separate studies in Figure 9(g),[32–35] this novel nomogram, which contained the platelet adhesion gene data, had good predictive power.

Expression validation of key genes

The expression of two key genes (POU6F1 and MATN3) in the regulatory network and two genes (ALOX12 and ACTG1) were further investigated in the clinical samples. The mRNA expression in normal and tumor tissues obtained from four COAD patients from real world was detected by RT-qPCR, and the protein expression in normal and tumor tissues obtained from four COAD patients from real world was detected by immunohistochemistry. As shown in Figure 7(g) and (h), the mRNA and protein expression levels of POU6F1 were significantly lower in tumor tissues, when compared to normal tissues, while the mRNA expression levels of MATN3 were not statistically different between these tissues. The expression of MATN3 protein was, however, statistically different. Furthermore, the mRNA and protein expression levels of ALOX12 were significantly lower in tumor tissues, when compared to normal tissues (Figure 9(c) and (d)), while the mRNA and protein expression levels of ACTG1 were significantly higher in tumor tissues, when compared to normal tissues (Figure 9(c) and (d)).

Discussion

Colon cancer rapidly progresses after initiation. Therefore, more effective drugs or therapeutic targets are required to

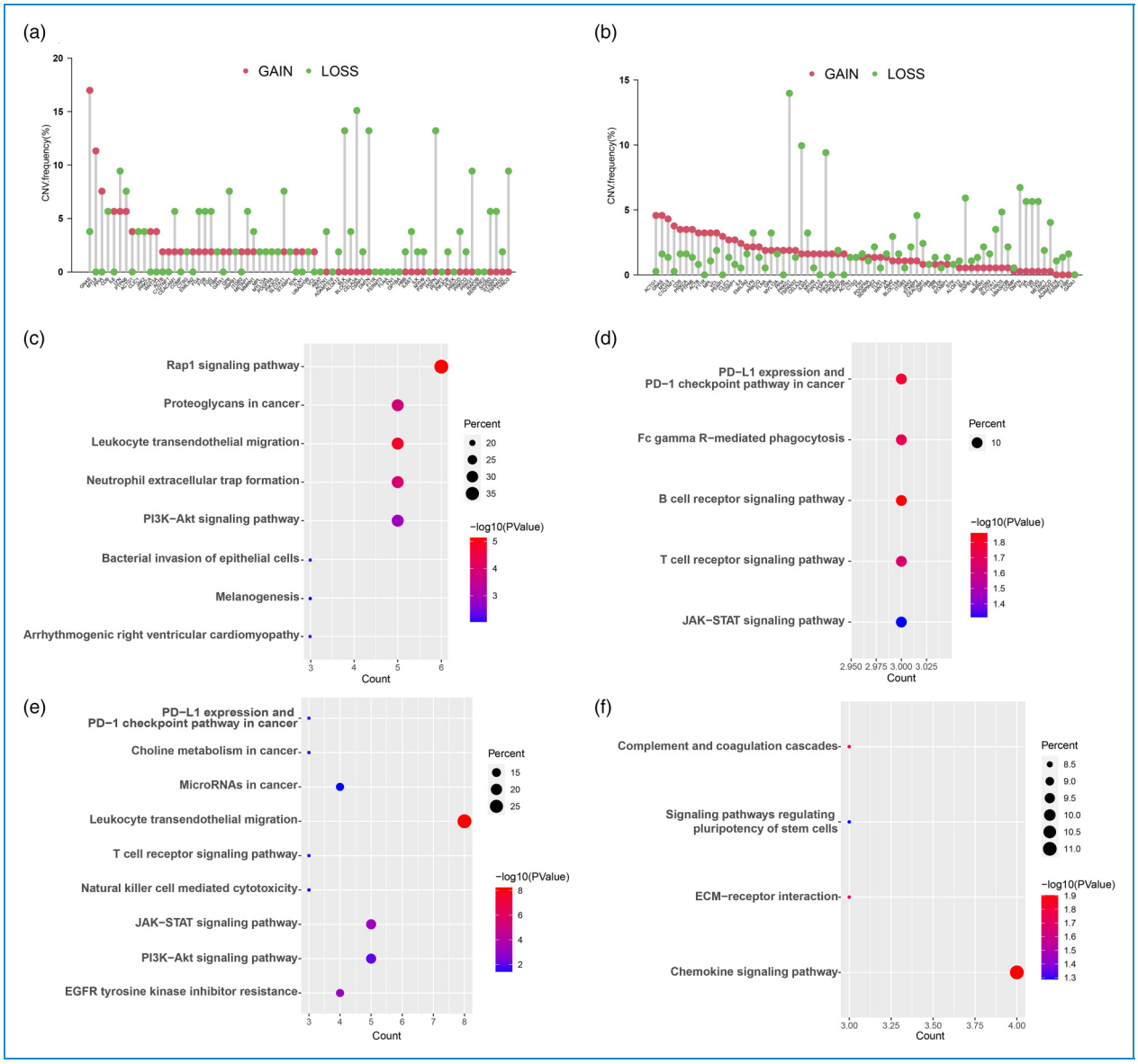

Figure 6. Copy number variation (CNV) and enrichment analysis in clusters. (a) CNV plots for Cluster1. (b) CNV plots for Cluster2. (c and d) Enrichment analysis for the copy number gain of genes (c) and loss of genes (d) in Cluster1. (e and f) Enrichment analysis for the copy number gain of genes (e) and loss of genes (f) in Cluster2.

improve the survival rate. Through the multidimensional analysis of tumors, it is possible to uncover the weaknesses of tumors and target these for treatment. There is increasing evidence that points to the involvement of platelets in the development of tumors.[2,36] The present study initially revealed that high platelet count is associated with poor OS. Using the data obtained from four large studies, it was found that the mutations, amplifications, profound deletions, and multiple alterations in these genes lead to poor survival.

Based on the DEGs associated with platelet adhesion, the COAD tumor expression matrix was further divided into two groups using NMF clustering analysis. The survival analysis of these data revealed that the patient survival rates were better in Cluster2, when compared to Cluster1. Normally, alterations to copy numbers are detrimental, and these may be contributing factors to various human diseases.[37] In the present study, 16 genes were identified to have more copy number increases than deletions in Cluster1, and 30 genes were identified to have more copy number deletions than increases. In Cluster2, 29 genes had more copy number increases than deletions, and 36 genes had more copy number deletions than increases. Next, an enrichment analysis was performed for these genes to gain a deeper understanding of the differences between the two clusters. It was found that the PI3K-Akt signaling pathway was present in

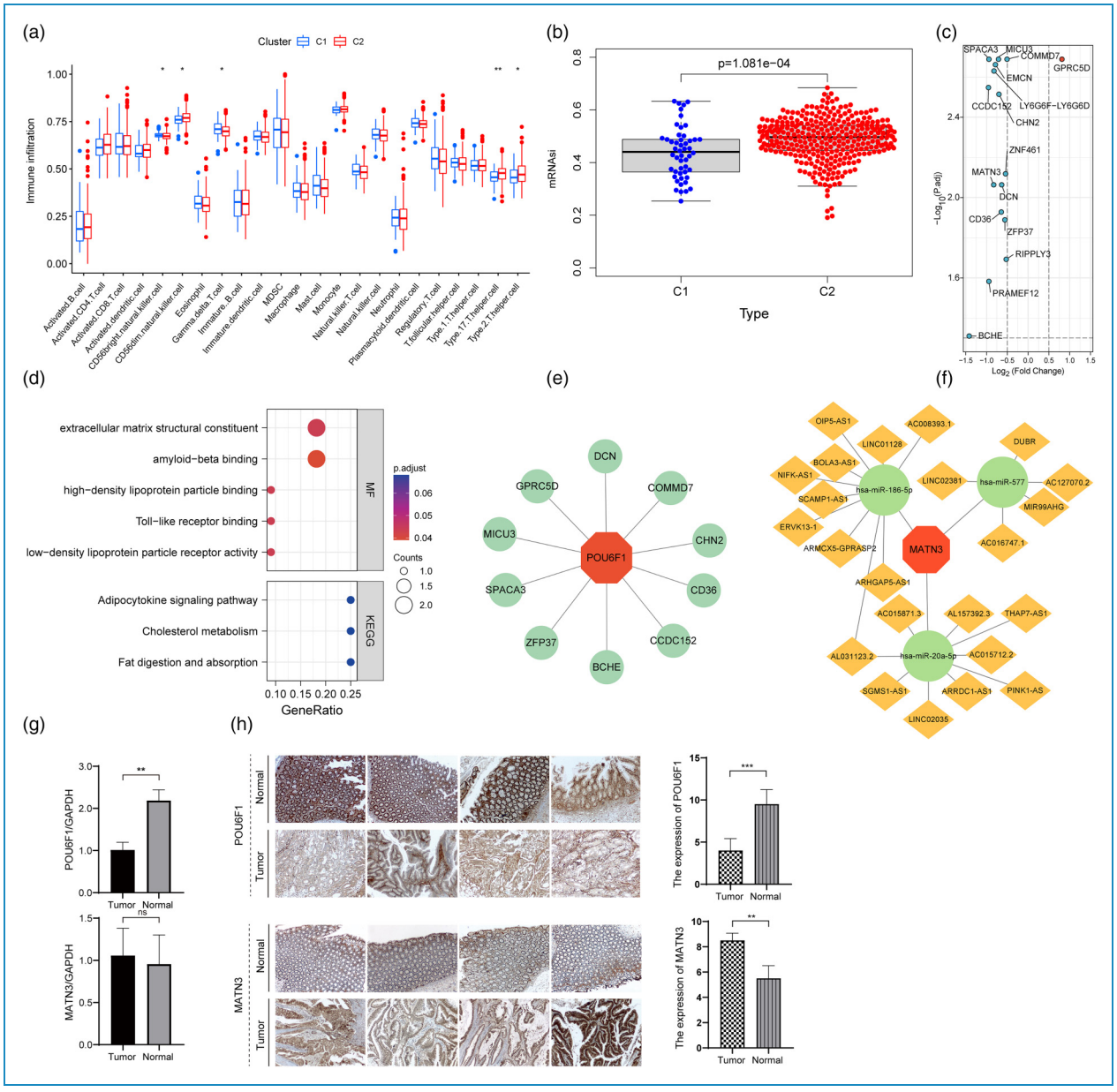

Figure 7. Profile of signatures of the 433 patients with COAD from TCGA and validation. (a) Difference in immune cell infiltration between the two clusters. (b) Difference in cancer stemness index between the two clusters. (c) Volcano plots for the hub genes. (d) GO and KEGG enrichment analysis for the hub genes. (e) Network of transcription factors. (f) Network for ceRNAs. (g) RT-qPCR results for POU6F1 or MATN3 expression at the mRNA level. (h) immunohistochemistry results were evaluated semiquantitatively for POU6F1 or MATN3 expression at the protein level.
RT-qPCR: real-time quantitative polymerase chain reaction; ceRNA: competing endogenous RNA; GO: gene ontology; KEGG: Kyoto Encyclopedia of Genes and Genomes.

both clusters in the copy number amplification groups, suggesting that platelet adhesion-related genes may play a role in the development of COAD through the PI3K-Akt signaling pathway. These results also revealed that platelet adhesion-related genes may be involved in the remodeling of the tumor immune microenvironment.

It is important to investigate the differences in immune cell infiltration between clusters, since tumor tissues contain stromal cells, fibroblasts, and immune cells, which all contribute to the tumor microenvironment.[38,39] A previous study revealed that the degree of immune cell infiltration in tumor tissues plays an important role in tumor development and treatment.[40] The results of the present study revealed that five immune cells were significantly different between the two groups: $CD56^{bright}$, $CD56^{dim}$, γδT cells, T_h17 cells, and T_h2 cells. These data

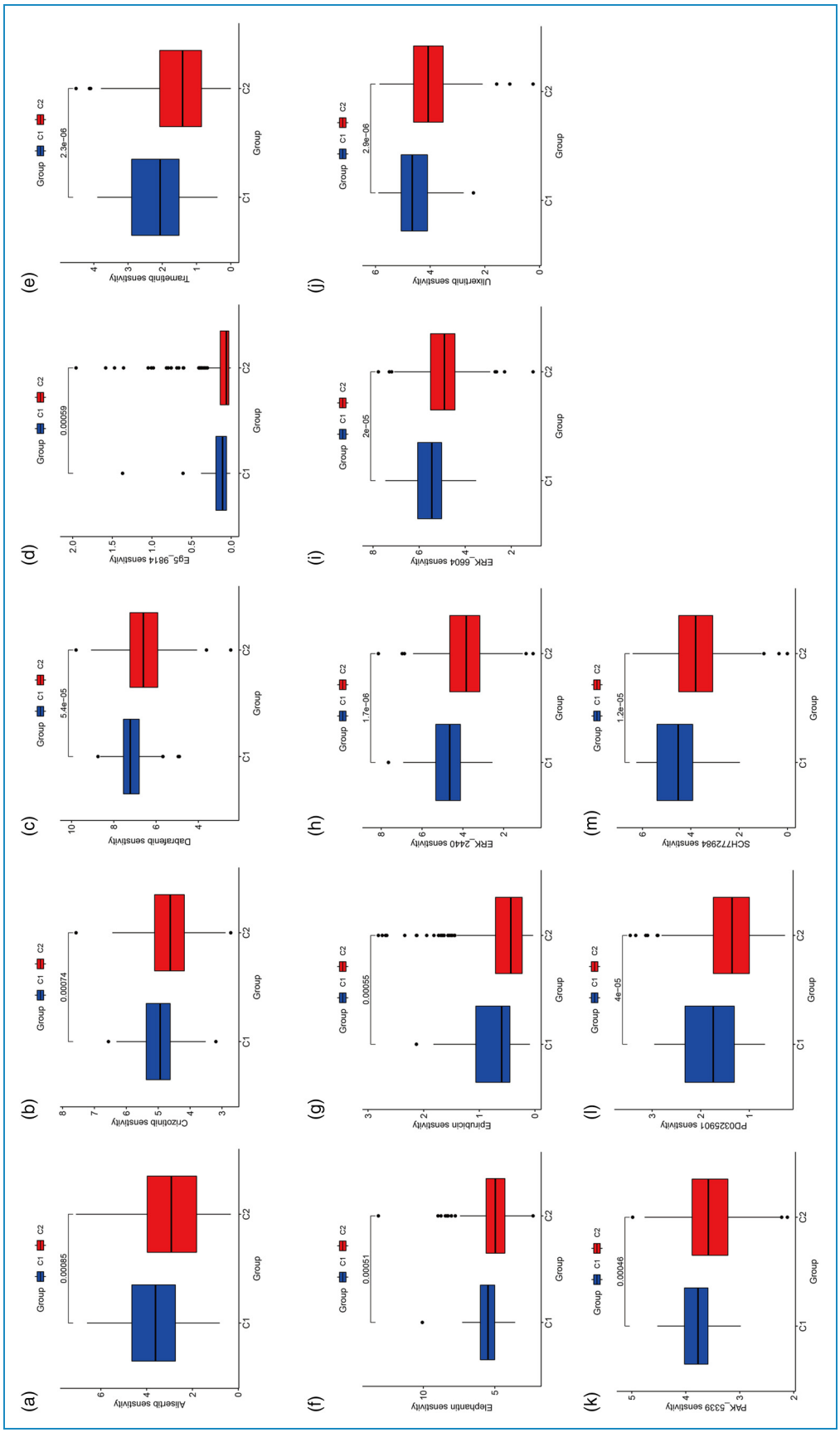

Figure 8. Significant differences identified in the drug sensitivity analysis: (a) alisertib, (b) crizotinib, (c) dabrafenib, (d) Eg5_9814, (e) trametinib, (f) elephantin, (g) epirubicin, (h) ERK_2440, (i) ERK_6604, (j) ulixertinib, (k) PAK_5339, (l) PD0325901, and (m) SCH772984 (refer to Table 1 for the drug mechanisms of action).

Table 1. Drugs with significant differences between the two clusters after the drug sensitivity analysis.

Drug	Antitumor mechanism	*P*
Alisertib	Alisertib has antitumor activity and induces apoptosis and autophagy by targeting the AKT/mTOR/AMPK/p38 pathway in leukemic cells.[23]	<0.001
Crizotinib	In vitro, Crizotinib was shown to be a potent inhibitor of tumor growth, through inhibition of tyrosine phosphorylation of NPM-ALK and tyrosine phosphorylation of c-Met.[24]	<0.001
Dabrafenib	Dabrafenib is an ATP-competitive Raf inhibitor.[25]	<0.001
Elephantin	Elephantin is a sesquiterpenoid tumor inhibitor.[26]	<0.001
Epirubicin	Epirubicin is a Foxp3 inhibitor that inhibits the inhibition of DNA and RNA synthesis.[27]	<0.001
PD0325901 (Mirdametinib)	PD0325901 is a selective and non-ATP-competitive MEK inhibitor that inhibits p-ERK1/2 expression and induces apoptosis.[28]	<0.001
SCH772984	CH772984 is a highly selective and ATP-competitive ERK inhibitor with antitumor activity.[29]	<0.001
Trametinib	Trametinib is a potent MEK inhibitor that activates tumor cell autophagy and induces apoptosis.[30]	<0.001
Ulixertinib	Ulixertinib is a highly selective and ATP-competitive ERK1/2 inhibitor that inhibits the phosphorylation of ERK2 and the downstream protein RSK.[31]	<0.001
Eg5_9814	GDSC database	<0.001
ERK_2440	GDSC database	<0.001
ERK_6604	GDSC database	<0.001
PAK_5339	GDSC database	<0.001

AKT/mTOR/AMPK: protein kinase B/mammalian target of rapamycin/AMP-protein activated protein kinase; NPM-ALK: nucleophosmin-anaplastic lymphoma kinase; ATP: adenosine triphosphate; MEK: mitogen-activated extracellular signal-regulated kinase; ERK: extracellular signal-regulated kinase; RSK: ribosomal S6 kinase.

were consistent with the enriched pathways, according to the CNV genes identified above. Combined with the survival analysis results for the two clusters, the increase in mature NK cells and T_h cells at the tumor site may be a breakthrough point to improve the immune microenvironment of COAD.

A small subset of cancer stem cells (CSCs) can self-renew, indefinitely proliferate and differentiate in multiple directions. These are the primordial cells responsible for tumorigenesis and recurrence.[41] Previous studies have revealed that CSCs are the most important cause of malignancy treatment failure. This is due to the tumorigenesis, and the phenotypic differences in the differentiated progeny of tumor cells. Furthermore, it was found that cancer stemness was higher in Cluster2, when compared to Cluster1. Moreover, the survival rates were better in Cluster2, when compared to Cluster1. This illustrates the complexity of the development process of COAD. In order to provide guidance in clinical medication, the two clusters were assessed for drug sensitivity. A total of 13 drugs were identified. These drugs have been or will be used in clinics for the treatment of tumors.

Next, the differences in gene expression between the two clusters were explored by performing an enrichment analysis. Interestingly, the GO and KEGG analysis results revealed that the identified hub genes were involved in lipid and cholesterol metabolism in COAD. A growing number of studies have demonstrated the importance of these two pathways in tumor development.[42–45] Meanwhile, the transcription factor pathway enrichment analysis of hub genes was performed using the DAVID tool to construct a transcription factor regulatory network. Transcription factors are important hubs that connect the signaling and protein expression in vivo. The construction of transcription factor regulatory networks among clusters can help in understanding the potential regulatory mechanism of platelet adhesion-related genes in COAD. The analysis revealed that 10 hub genes were enriched in POU6F1, which is a member of the POU factor family of transcription factors.[46] Interestingly, in the present study, POU6F1 was identified to have a low

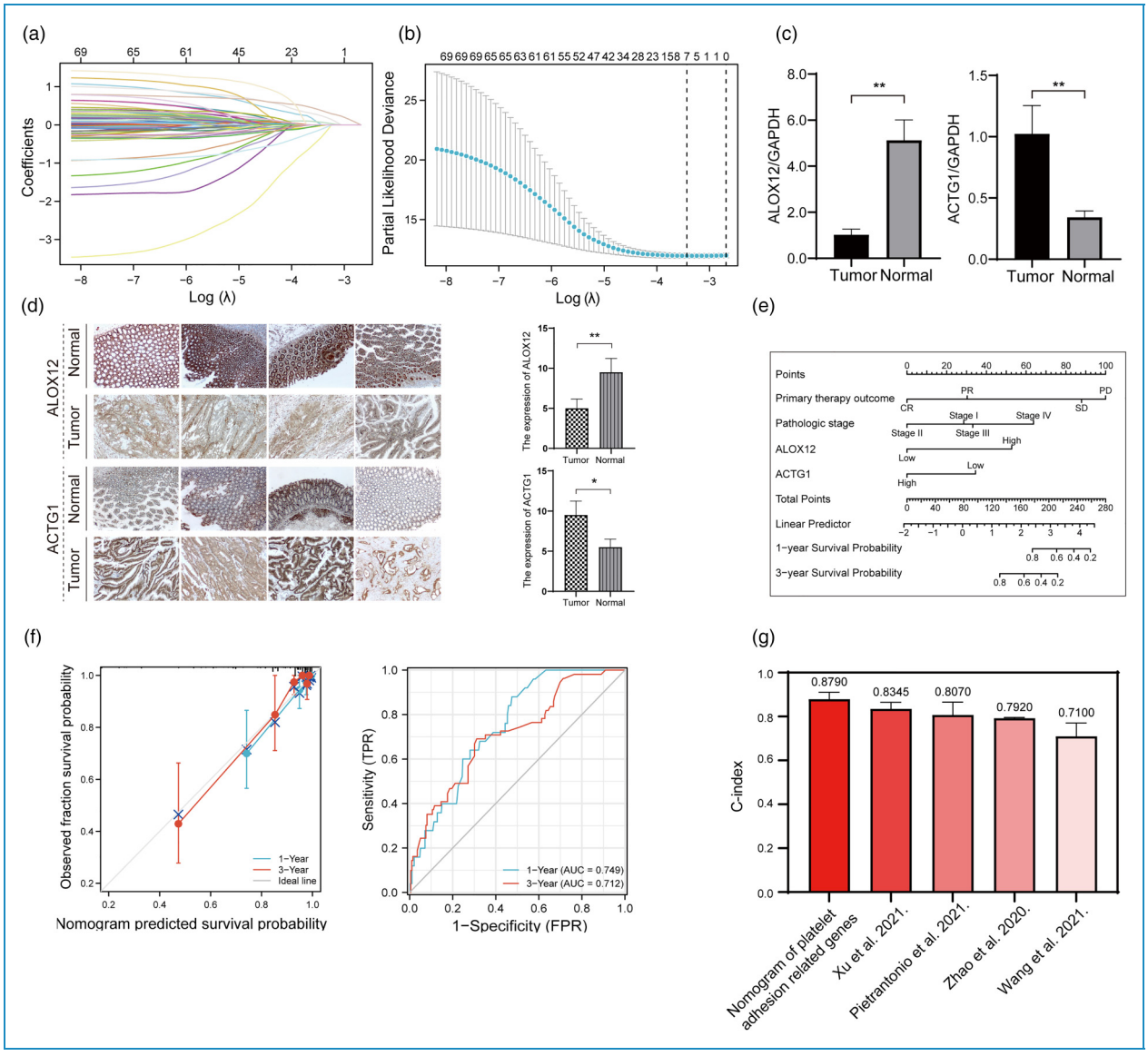

Figure 9. Construction and verification of the nomogram. (a) Plots for the LASSO regression coefficients over the different values of the penalty parameter. (b) The LASSO regression analysis result. (c) RT-qPCR results for ALOX12 or ACTG1 expression at the mRNA level. (d) immunohistochemistry results were evaluated semiquantitatively for ALOX12 or ACTG1 expression at the protein level. (e) Nomogram for OS. (f) Calibration plots for the nomogram, and ROC curves for the nomogram. (g) Comparison of prognostic models in the different studies.

CR: complete response; PR: partial response; SD: stable disease; PD: progressive disease; LASSO: least absolute shrinkage and selection operator; RT-qPCR: real-time quantitative polymerase chain reaction; OS: overall survival; ROC: receiver operating characteristic.

expression in tumor tissues, when compared to normal tissues. Another study reported that downregulation of POU6F1 in lung adenocarcinoma (LUAD) is associated with poor prognosis.[47] The enrichment results revealed that platelet adhesion-related genes may be involved in the regulation of gene expression, providing novel insights into the treatment of COAD. However, further experimental investigations are required.

In order to elucidate the potential regulatory mechanisms of ceRNA in COAD, another ceRNA regulatory network was constructed to identify new therapeutic targets at the lncRNA–miRNA–mRNA level. A survival analysis was conducted for all hub genes, and three relevant miRNAs and 23 lncRNAs were obtained in MATN3 as a single target gene. The MATN3 gene encodes a member of the von Willebrand factor A domain, and this has been considered to be involved in the formation of filamentous networks in extracellular matrices.[48] Furthermore, the MATN3 gene has received increasing attention in recent years, especially in gastric cancer research, due to its

potential to serve as both a diagnostic biomarker and a prognostic biomarker.[49–51] Moreover, MATN3 acts as an oncogenic factor in gastric cancer, which is in agreement with the findings of the present study. Although the MATN3 expression was not statistically different in the COAD and normal tissues, treatments that target MATN3 can be a promising therapeutic strategy for other cancers. Unfortunately, the mechanism, in which the MATN3 gene influences cancer development and progression, has received minimal attention to date.

Meanwhile, the miRNAs and lncRNAs identified in the present study have received increasing attention in tumor research. Hsa-mir-577 has been mentioned in several studies,[52–55] but this appears to have a dual nature, depending on the cancer type. Atypical endometrial hyperplasia may be associated with the aberrant expression of hsa-miR-577, which targets IGF1 and IGF1R, while it was found that hsa-miR-577 significantly downregulates the translation efficiency of CYP3A4 mRNA in the liver.[55,56] A study reported that the downregulation of hsa-mir-20a-5p by atorvastatin can increase the low-density lipoprotein receptor (LDLR) mRNA and protein expression in HepG2 cells, while the overexpression of has-mir-20a-5p can reduce the LDLR mRNA and protein expression.[57] In another study on COAD, hsa-mir-186-5p was described as a tumor suppressive factor that inhibits the SMAD6 and SMAD7 expression, thereby regulating the tumor growth factor-β signaling pathway.[58]

lncRNAs can serve as diagnostic biomarkers for a variety of cancers. Four lncRNAs (ARRDC1-AS1, OIP5-AS1, BOLA3-AS1, and NIFK-AS1) were mentioned in previous COAD studies.[59–62] Collectively, these factors may lead to the further exploration of COAD progression and can be investigated as biomarkers and therapeutic targets for COAD.

DUBR, MIR99AHG, PINK1-AS, SGMS1-AS1, LINC01128, and SCAMP1-AS1 were investigated in LUAD.[63–68] Furthermore, it was reported that ARHGAP5-AS1 is upregulated in chemoresistant gastric cancer cells and that the knockdown of the lncRNA reverses the resistance.[69] AL031123.2 can be used as a prognostic factor in cervical cancer.[70] There is a significant correlation between the AL157392.3 expression and glycolysis across a wide range of cancers.[71] THAP7-AS1 is significantly upregulated in gastric cancer tissues, when compared to non-tumorous gastric tissues.[72] However, the specific mechanistic role of these aforementioned lncRNAs in COAD remains unclear. Thus, more in-depth experimental studies are required.

Finally, in the LASSO logistic regression analysis, two prognostic factors (ALOX12 and ACTG1) were identified. The ALOX12 gene encodes a member of the lipoxygenase family of proteins. This encoded enzyme acts on different polyunsaturated fatty acid substrates to generate bioactive lipid mediators, including eicosanoids and lipoxins.[73] Interestingly, ALOX12 is a pro-oncogenic factor, which may promote tumor development through lipid metabolic pathways, and this has been confirmed in several studies.[74,75] In addition, ACTG1 is associated with cell migration and adhesion.[76] The clinical utility of the nomogram was demonstrated using ROC curves and calibration plots. The calibration plots and ROC curves of the nomogram were well-calibrated.

The present study had several limitations. First, further validation of the efficacy and standardization of the two clusters in clinical diagnosis is necessary, but remains challenging. Second, the present study lacked experimental studies on platelet adhesion in patients. Finally, the multidimensional analysis results for platelet-associated adhesion genes had significant practical implications. Therefore, there is an urgent need to further explore existing results, in order to identify novel treatment options for COAD, which could not be completed in the present study.

Conclusion

Based on the presented data, it was revealed that the effects of platelet adhesion-related genes in COAD are complex. On the one hand, platelet adhesion-related genes can affect the OS of COAD patients by regulating lipid and cholesterol metabolism, which may be caused by the differences in CNVs. On the other hand, several immune cells have varying degrees of infiltration, according to the different platelet adhesion-related gene expression levels, which may cause the tumors of different patients to respond differently to the same drug. Finally, the constructed nomogram can be used as a reference in clinical practice.

Acknowledgements: We would like to thank all participants for their contribution to the study, and the free use of The Cancer Genome Atlas (TCGA) database.

Contributorship: XJC and YBS: study conception; XJC, DHL, LQW, XA, ZZF, and XHL: data analysis; LQW: data curation; DHL: project administration; DL: review of experimental data; CH: writing/review and editing; XJC and YBS: writing of the manuscript. All authors have read and agreed to the published version of the manuscript.

Declaration of conflicting interests: The authors declared no potential conflicts of interest with respect to the research, authorship, and/or publication of this article.

Ethical approval: The study was approved by the First Affiliated Hospital of Guangxi Medical University (No. 2023-E186-02).

Data availability statement: The data is available from the corresponding authors upon reasonable request.

Funding: The authors disclosed receipt of the following financial support for the research, authorship, and/or publication of this article: This work was supported by the Guangxi Health Department Research Project, Students' Program for Innovation and Entrepreneurship of Guangxi Medical University, Clinical Research "Climbing" Program of the First Affiliated Hospital of Guangxi Medical University, Promoting Project of Basic Capacity for Young and Middle-aged University Teachers in Guangxi (grant numbers z20190853, X202210598339, YYZS2020023, and 020KY03016).

Guarantor: Xiao-jv Chi.

ORCID iDs: Xiao-jv Chi https://orcid.org/0000-0002-2450-4858
Xin An https://orcid.org/0000-0002-0944-7365

Supplemental material: Supplemental material for this article is available online.

References

1. Hinterleitner C, Strahle J, Malenke E, et al. Platelet PD-L1 reflects collective intratumoral PD-L1 expression and predicts immunotherapy response in non-small cell lung cancer. *Nat Commun* 2021; 12: 7005.
2. Mammadova-Bach E, Gil-Pulido J, Sarukhanyan E, et al. Platelet glycoprotein VI promotes metastasis through interaction with cancer cell-derived galectin-3. *Blood* 2020; 135: 1146–1160.
3. Arakawa Y, Miyazaki K, Yoshikawa M, et al. Value of the fibrinogen-platelet ratio in patients with resectable pancreatic cancer. *J Med Invest* 2021; 68: 342–346.
4. Kizer NT, Hatem H, Nugent EK, et al. Chemotherapy response rates among patients with endometrial cancer who have elevated serum platelets. *Int J Gynecol Cancer* 2015; 25: 1015–1022.
5. Li R, Ren M, Chen N, et al. Presence of intratumoral platelets is associated with tumor vessel structure and metastasis. *BMC Cancer* 2014; 14: 167.
6. Dovizio M, Ballerini P, Fullone R, et al. Multifaceted functions of platelets in cancer: From tumorigenesis to liquid biopsy tool and drug delivery system. *Int J Mol Sci* 2020; 21: 9585.
7. Guo Y, Cui W, Pei Y, et al. Platelets promote invasion and induce epithelial to mesenchymal transition in ovarian cancer cells by TGF-beta signaling pathway. *Gynecol Oncol* 2019; 153: 639–650.
8. Lathouras K, Panagakis G, Bowden SJ, et al. Diagnostic value of post-operative platelet-to-white blood cell ratio after splenectomy in patients with advanced ovarian cancer. *Int J Gynecol Cancer* 2019; 29: 1292–1297.
9. Krenn-Pilko S, Langsenlehner U, Thurner EM, et al. The elevated preoperative platelet-to-lymphocyte ratio predicts poor prognosis in breast cancer patients. *Br J Cancer* 2014; 110: 2524–2530.
10. Baranyai Z, Krzystanek M, Josa V, et al. The comparison of thrombocytosis and platelet-lymphocyte ratio as potential prognostic markers in colorectal cancer. *Thromb Haemost* 2014; 111: 483–490.
11. Calverley DC, Phang TL, Choudhury QG, et al. Significant downregulation of platelet gene expression in metastatic lung cancer. *Clin Transl Sci* 2010; 3: 227–232.
12. Kilincalp S, Ekiz F, Basar O, et al. Mean platelet volume could be possible biomarker in early diagnosis and monitoring of gastric cancer. *Platelets* 2014; 25: 592–594.
13. Osada J, Rusak M, Kamocki Z, et al. Platelet activation in patients with advanced gastric cancer. *Neoplasma* 2010; 57: 145–150.
14. Sanchez Ramirez J, Bequet-Romero M, Morera Diaz Y, et al. Does VEGF-targeted active immunotherapy induce complete abrogation of platelet VEGF levels? *BMC Res Notes* 2019; 12: 323.
15. Braun LJ, Stegmeyer RI, Schafer K, et al. Platelets docking to VWF prevent leaks during leukocyte extravasation by stimulating Tie-2. *Blood* 2020; 136: 627–639.
16. Anvari S, Osei E and Maftoon N. Interactions of platelets with circulating tumor cells contribute to cancer metastasis. *Sci Rep* 2021; 11: 15477.
17. Chivukula VK, Krog BL, Nauseef JT, et al. Alterations in cancer cell mechanical properties after fluid shear stress exposure: A micropipette aspiration study. *Cell Health Cytoskelet* 2015; 7: 25–35.
18. Romero-Moreno R, Curtis KJ, Coughlin TR, et al. The CXCL5/CXCR2 axis is sufficient to promote breast cancer colonization during bone metastasis. *Nat Commun* 2019; 10: 4404.
19. Qi C, Li B, Guo S, et al. P-selectin-mediated adhesion between platelets and tumor cells promotes intestinal tumorigenesis in apc(min/+) mice. *Int J Biol Sci* 2015; 11: 679–687.
20. Zaccaria S and Raphael BJ. Accurate quantification of copy-number aberrations and whole-genome duplications in multi-sample tumor sequencing data. *Nat Commun* 2020; 11: 4301.
21. Satas G, Zaccaria S, Mon G, et al. SCARLET: Single-cell tumor phylogeny inference with copy-number constrained mutation losses. *Cell Syst* 2020; 10: 323–332 e328.
22. Yang W, Soares J, Greninger P, et al. Genomics of Drug Sensitivity in Cancer (GDSC): A resource for therapeutic biomarker discovery in cancer cells. *Nucleic Acids Res* 2013; 41: D955–D961.
23. Vagiannis D, Zhang Y, Budagaga Y, et al. Alisertib shows negligible potential for perpetrating pharmacokinetic drug-drug interactions on ABCB1, ABCG2 and cytochromes P450, but acts as dual-activity resistance modulator through the inhibition of ABCC1 transporter. *Toxicol Appl Pharmacol* 2022; 434: 115823.
24. Schöffski P, Kubickova M, Wozniak A, et al. Long-term efficacy update of crizotinib in patients with advanced, inoperable inflammatory myofibroblastic tumour from EORTC trial 90101 CREATE. *Eur J Cancer* 2021; 156: 12–23.
25. Birden N, Selvi Gunel N, Ozates NP, et al. The effects of epigallocatechin-3-gallate and dabrafenib combination on apoptosis and the genes involved in epigenetic events in anaplastic thyroid cancer cells. *Med Oncol* 2022; 39: 98.
26. Kupchan SM, Aynehchi Y, Cassady JM, et al. Tumor inhibitors XL. The isolation and structural elucidation of elephantin and elephantopin, two novel sesquiterpenoid tumor inhibitors from *Elephantopus elatus*. *J Org Chem* 1969; 34: 3867–3875.

27. Shen LW, Jiang XX, Li ZQ, et al. Cepharanthine sensitizes human triple negative breast cancer cells to chemotherapeutic agent epirubicin via inducing cofilin oxidation-mediated mitochondrial fission and apoptosis. *Acta Pharmacol Sin* 2022; 43: 177–193.
28. Weiss BD, Wolters PL, Plotkin SR, et al. NF106: A neurofibromatosis clinical trials consortium phase ii trial of the MEK inhibitor mirdametinib (pd-0325901) in adolescents and adults with nf1-related plexiform neurofibromas. *J Clin Oncol* 2021; 39: 797–806.
29. Kopczynski M, Rumienczyk I, Kulecka M, et al. Selective extracellular signal-regulated kinase 1/2 (erk1/2) inhibition by the sch772984 compound attenuates in vitro and in vivo inflammatory responses and prolongs survival in murine sepsis models. *Int J Mol Sci* 2021; 22: 10204.
30. Vigoda M, Mathieson C, Evans N, et al. Functional proteomics of patient derived head and neck squamous cell carcinoma cells reveal novel applications of trametinib. *Cancer Biol Ther* 2022; 23: 310–318.
31. Wu J, Liu D, Offin M, et al. Characterization and management of ERK inhibitor associated dermatologic adverse events: Analysis from a nonrandomized trial of ulixertinib for advanced cancers. *Invest New Drugs* 2021; 39: 785–795.
32. Xu R, Zhou B, Hu P, et al. Development and validation of prognostic nomograms for patients with colon neuroendocrine neoplasms. *World J Surg Oncol* 2021; 19: 233.
33. Pietrantonio F, Fuca G, Manca P, et al. Validation of the colon life nomogram in patients with refractory metastatic colorectal cancer enrolled in the RECOURSE trial. *Tumori* 2021; 107: 353–359.
34. Zhao B, Gabriel RA, Vaida F, et al. Using machine learning to construct nomograms for patients with metastatic colon cancer. *Colorectal Dis* 2020; 22: 914–922.
35. Wang S, Liu Y, Shi Y, et al. Development and external validation of a nomogram predicting overall survival after curative resection of colon cancer. *J Int Med Res* 2021; 49: 3000605211015023.
36. Malehmir M, Pfister D, Gallage S, et al. Platelet GPIbalpha is a mediator and potential interventional target for NASH and subsequent liver cancer. *Nat Med* 2019; 25: 641–655.
37. Li Y, Liu Y, Xu H, et al. Heterozygous deletion of chromosome 17p renders prostate cancer vulnerable to inhibition of RNA polymerase II. *Nat Commun* 2018; 9: 4394.
38. Kolb D, Kolishetti N, Surnar B, et al. Metabolic modulation of the tumor microenvironment leads to multiple checkpoint inhibition and immune cell infiltration. *ACS Nano* 2020; 14: 11055–11066.
39. Li J, Byrne KT, Yan F, et al. Tumor cell-intrinsic factors underlie heterogeneity of immune cell infiltration and response to immunotherapy. *Immunity* 2018; 49: 178–193 e177.
40. Tobin JWD, Keane C, Gunawardana J, et al. Progression of disease within 24 months in follicular lymphoma is associated with reduced intratumoral immune infiltration. *J Clin Oncol* 2019; 37: 3300–3309.
41. Sharma VP, Tang B, Wang Y, et al. Live tumor imaging shows macrophage induction and TMEM-mediated enrichment of cancer stem cells during metastatic dissemination. *Nat Commun* 2021; 12: 7300.
42. Zhang C, Zhu N, Li H, et al. New Dawn for cancer cell death: Emerging role of lipid metabolism. *Mol Metab* 2022; 63: 101529.
43. Huang J, Wang J, He H, et al. Close interactions between lncRNAs, lipid metabolism and ferroptosis in cancer. *Int J Biol Sci* 2021; 17: 4493–4513.
44. Kosaka S, Miyashita M, McNamala K, et al. Bird's eye view analysis of in situ cholesterol metabolic pathways in breast cancer patients and its clinicopathological significance in their subtypes. *J Steroid Biochem Mol Biol* 2022; 221: 106103.
45. Xu H, Zhou S, Tang Q, et al. Cholesterol metabolism: New functions and therapeutic approaches in cancer. *Biochim Biophys Acta Rev Cancer* 2020; 1874: 188394.
46. Li WY, Li ZG, Fu XM, et al. Transgenic Schwann cells overexpressing POU6F1 promote sciatic nerve regeneration within acellular nerve allografts. *J Neural Eng* 2022; 19: 066006.
47. Xiao W, Geng W, Zhou M, et al. POU6F1 Cooperates with RORA to suppress the proliferation of lung adenocarcinoma by downregulation HIF1A signaling pathway. *Cell Death Dis* 2022; 13: 427.
48. Vincourt JB, Etienne S, Grossin L, et al. Matrilin-3 switches from anti- to pro-anabolic upon integration to the extracellular matrix. *Matrix Biol* 2012; 31: 290–298.
49. Li D, Xu J, Dong X, et al. Diagnostic and prognostic value of MATN3 expression in gastric carcinoma: TCGA database mining. *J Gastrointest Oncol* 2021; 12: 1374–1383.
50. Zhang C, Liang Y, Ma MH, et al. KRT15, INHBA, MATN3, and AGT are aberrantly methylated and differentially expressed in gastric cancer and associated with prognosis. *Pathol Res Pract* 2019; 215: 893–899.
51. Wei C, Li M, Lin S, et al. Characterization of tumor mutation burden-based gene signature and molecular subtypes to assist precision treatment in gastric cancer. *Biomed Res Int* 2022; 2022: 4006507.
52. Cao Y, Ye D, Shen Z, et al. The expression profile, clinical application and potential tumor suppressing mechanism of hsa_circ_0001675 in head and neck carcinoma. *Front Oncol* 2022; 12: 769666.
53. Yang J, Cong X, Ren M, et al. Circular RNA hsa_circrna_0007334 is predicted to promote MMP7 and COL1A1 expression by functioning as a miRNA sponge in pancreatic ductal adenocarcinoma. *J Oncol* 2019; 2019: 7630894.
54. Ren ZP, Hou XB, Tian XD, et al. Identification of nine microRNAs as potential biomarkers for lung adenocarcinoma. *FEBS Open Bio* 2019; 9: 315–327.
55. Wei Z, Jiang S, Zhang Y, et al. The effect of microRNAs in the regulation of human CYP3A4: A systematic study using a mathematical model. *Sci Rep* 2014; 4: 4283.
56. Tang S and Dai Y. RNA Sequencing reveals significant miRNAs in atypical endometrial hyperplasia. *Eur J Obstet Gynecol Reprod Biol* 2018; 225: 129–135.
57. Saavedra K, Leal K, Saavedra N, et al. Microrna-20a-5p downregulation by atorvastatin: A potential mechanism involved in lipid-lowering therapy. *Int J Mol Sci* 2022; 23: 5022.
58. Bayat Z, Ghaemi Z, Behmanesh M, et al. Hsa-miR-186-5p regulates TGFbeta signaling pathway through expression suppression of SMAD6 and SMAD7 genes in colorectal cancer. *Biol Chem* 2021; 402: 469–480.
59. Cai HJ, Zhuang ZC, Wu Y, et al. Development and validation of a ferroptosis-related lncRNAs prognosis signature in colon cancer. *Bosn J Basic Med Sci* 2021; 21: 569–576.

60. Xia F, Yan Y and Shen C. A prognostic pyroptosis-related lncRNAs risk model correlates with the immune microenvironment in colon adenocarcinoma. *Front Cell Dev Biol* 2021; 9: 811734.
61. Guo JN, Xia TY, Deng SH, et al. Prognostic immunity and therapeutic sensitivity analyses based on differential genomic instability-associated lncRNAs in left- and right-sided colon adenocarcinoma. *Front Mol Biosci* 2021; 8: 668888.
62. Tang Q, Hu X, Guo Q, et al. Discovery and validation of a novel metastasis-related lncRNA prognostic signature for colorectal cancer. *Front Genet* 2022; 13: 704988.
63. Nie W, Hu MJ, Zhang Q, et al. DUBR Suppresses migration and invasion of human lung adenocarcinoma cells via ZBTB11-mediated inhibition of oxidative phosphorylation. *Acta Pharmacol Sin* 2022; 43: 157–166.
64. Han C, Li H, Ma Z, et al. MIR99AHG is a noncoding tumor suppressor gene in lung adenocarcinoma. *Cell Death Dis* 2021; 12: 424.
65. Luo K, Xu S, Zhao J, et al. Upregulation of lncRNA pink1-as predicts the distant metastasis of patients with small cell lung cancer. *Mol Biotechnol* 2023; 65: 28–33.
66. Liu T, Yang C, Wang W, et al. LncRNA SGMS1-AS1 regulates lung adenocarcinoma cell proliferation, migration, invasion, and EMT progression via miR-106a-5p/MYLI9 axis. *Thorac Cancer* 2021; 12: 2104–2112.
67. Ding D, Zhang J, Luo Z, et al. Analysis of the lncRNA–miRNA–mRNA network reveals a potential regulatory mechanism of EGFR-TKI resistance in NSCLC. *Front Genet* 2022; 13: 851391.
68. Hao X, Li W, Li W, et al. Re-evaluating the need for mediastinal lymph node dissection and exploring lncRNAs as biomarkers of N2 metastasis in T1 lung adenocarcinoma. *Transl Lung Cancer Res* 2022; 11: 1079–1088.
69. Zhu L, Zhu Y, Han S, et al. Impaired autophagic degradation of lncRNA ARHGAP5-AS1 promotes chemoresistance in gastric cancer. *Cell Death Dis* 2019; 10: 383.
70. Chen P, Gao Y, Ouyang S, et al. A prognostic model based on immune-related long non-coding RNAs for patients with cervical cancer. *Front Pharmacol* 2020; 11: 585255.
71. Ho KH, Huang TW, Shih CM, et al. Glycolysis-associated lncRNAs identify a subgroup of cancer patients with poor prognoses and a high-infiltration immune microenvironment. *BMC Med* 2021; 19: 59.
72. Liu HT, Zou YX, Zhu WJ, et al. lncRNA THAP7-AS1, transcriptionally activated by SP1 and post-transcriptionally stabilized by METTL3-mediated m6A modification, exerts oncogenic properties by improving CUL4B entry into the nucleus. *Cell Death Differ* 2022; 29: 627–641.
73. Baranowska M, Koziara Z, Suliborska K, et al. Interactions between polyphenolic antioxidants quercetin and naringenin dictate the distinctive redox-related chemical and biological behaviour of their mixtures. *Sci Rep* 2021; 11: 12282.
74. Huang Z, Xia L, Zhou X, et al. ALOX12 Inhibition sensitizes breast cancer to chemotherapy via AMPK activation and inhibition of lipid synthesis. *Biochem Biophys Res Commun* 2019; 514: 24–30.
75. Yang F, Zhang Y, Ren H, et al. Ischemia reperfusion injury promotes recurrence of hepatocellular carcinoma in fatty liver via ALOX12-12HETE-GPR31 signaling axis. *J Exp Clin Cancer Res* 2019; 38: 489.
76. Liu Y, Zhang Y, Wu H, et al. miR-10a suppresses colorectal cancer metastasis by modulating the epithelial-to-mesenchymal transition and anoikis. *Cell Death Dis* 2017; 8: e2739.